

Supporting information for

# Multi-feature round silicon membrane filters enable fractionation and analysis of small micro- and nanoplastics with Raman spectroscopy and nano-FTIR

Michaela Meyns,<sup>1</sup> Frank Dietz,<sup>2</sup> Carin-Sonja Weinhold,<sup>2</sup> Heiko Züge,<sup>2</sup> Saskia Finckh,<sup>1,3</sup> Gunnar Gerdts<sup>1\*</sup>

1 Alfred-Wegener-Institute, Helmholtz centre for polar and marine research, Heligoland, Germany

2 Fraunhofer Institute for Silicon technology ISIT, Itzehoe, Germany

3 current address: UFZ Helmholtzzentrum für Umweltforschung, Leipzig, Germany

\*email address: gunnar.gerds@awi.de

## 1. PS and PMMA particle purification

Of each original particle dispersion 100  $\mu\text{L}$  were added into separate Vivaspin 2 centrifuge filter units that already contained 100  $\mu\text{L}$  of fresh ultrapure water (MilliQ, 18 M $\Omega$ ). After adding 300  $\mu\text{L}$  of ultrapure water, the samples were centrifuged at 5000 rpm/4923 g in a Sovall RC 26 Plus centrifuge (Dupont) with GSA holder at 18-19°C for 5 minutes with the brake off. Fresh ultrapure water was added until 500  $\mu\text{L}$  and the dispersion mixed by 5 s of ultrasound bath and pumping with a glass pipette inside the solution. After two minutes at 2000 rpm, the samples were redispersed again in pure ethanol before a final spin at 2000 rpm for 1 minute and dispersion in 1 mL of pure ethanol (ROTISOLV HPLC Gradient Grade 99.9%, Carl Roth). In the case of PMMA spheres, the first centrifugation was carried out at 2000 rpm for two minutes. Afterwards, 1 mL of ethanol was added followed by 3 minutes rotation at 1000 rpm and dispersion in 1 mL ethanol. Short ultrasound treatment was preferred over shaking and vortexing, as it was most reliable in dispersing the particles in aqueous and ethanol solution. Figure S1 illustrates this for the case of untreated commercial PE particles dispersed in water.

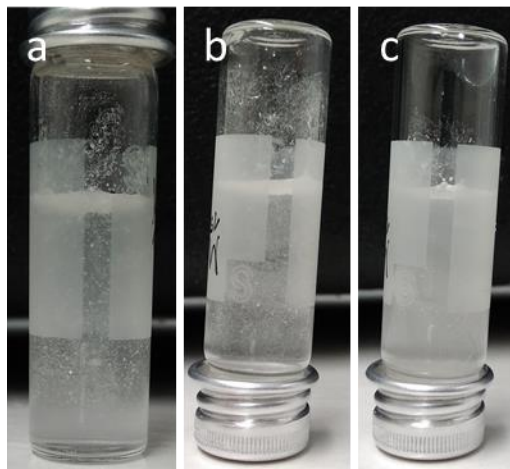


**Figure S1.** PE micro- and nanoparticles in water. a) initial, after vortexing b) after strong shaking and c) after 5 x 2 seconds ultrasound treatment by dipping the lower part into an ultrasonic bath.

## 2. Filtration unit

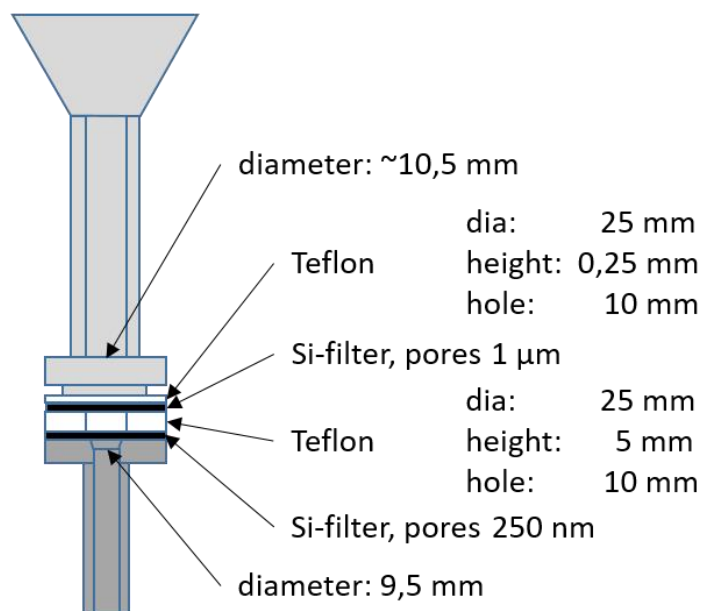


**Figure S2.** Photograph and drawing of filtration unit with two silicon filter membranes separated by a Teflon spacer. The type of glass funnel is often applied for filtration with Au-coated PC membranes that are spanned by a metal ring. For this reason, the glass has a lower diameter at the point of contact with the Teflon ring, which was found beneficial for preventing leakages.

### 3. Si membrane filter fabrication

Process Flow and tools used to fabricate silicon filter devices		
level	process/section	process relevant equipment
0	Transfer of the wafers to the front-end clean room of the industry partner, laser marking and cleaning	
1	cleaning and dry oxidation of the wafers	ASM400 oven system
	oxid layer thickness measurement	by ellipsometry
	lithography, dry structuring of the oxide, removal of the resist	spin coater for positive i-line resist, Canon i-line stepper, Applied Materials dryetching platform
2	lp-oven assisted deposition of 1,8µm amorphous Silicon	ASM400 oven system
	amorphous Silicon layer thickness measurement	by ellipsometry
	DUV-lithography of filter area with holes	Canon DUV cluster
	transfer into Fraunhofer MEMS-cleanroom	
	CDSEM analyses	CD-SEM Hitachi 9260A
	structuring of amorphous Silicon by Bosch deep reactive-ion etching	Lam Alliance with TCP9400 DSIE chamber
	removal of resist by dry ashing, RCA-cleaning	Gasonics L3510 dry asher, Semsysco SAP
3	turn over of process wafers	SPS 8" wafer transfer tool
	transfer to MEMS labor 2, grinding to 350µm, cleaning	grinder DISCO DFG 8540
	transfer into Fraunhofer MEMS-cleanroom, RCA cleaning and turn over of process wafers	Semsysco SAP, SPS 8" wafer transfer tool
4	lithography with 10 µm AZ-resist	SVG spin coater and developer, Suess Mask Aligner MA200,
	etching trough bulk silicon wafer by Bosch deep reactive-ion etching, removal of the resist	STS Pegasus, Gasonics L3510 dry asher,
	rca, turn over wafers,	
	oven annealing	Koyo VF-1000LP
5	RCA, deposition of 2*800 nm Al protection layer by physical deposition	Balzers BAK 760
	transfer, dicing on tape, return into Cleanroom	Disco DFD 6340
	manual separation of devices	
	Al etching in PWS	Ramgraber Bench
	manual RCA	Ramgraber Bench
	oxid etch in HF	RamgraberAutomatic Bench
	Descum	Gasonics L3510 dry asher
	final inspection	

#### 4. Si membrane filters

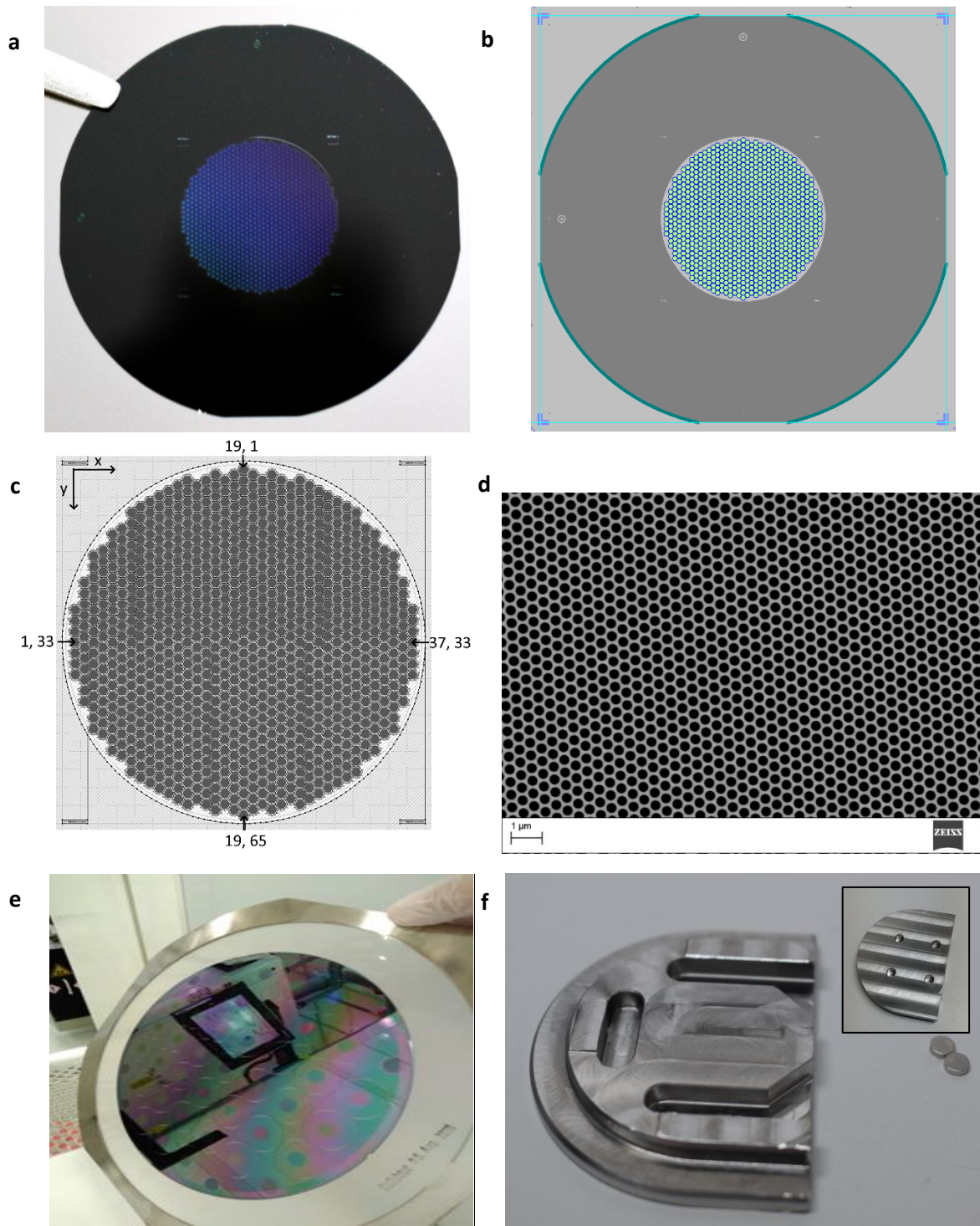


**Figure S3.** a) Photograph and b) technical drawing with circular orientation guides top and left and lithography markers positioned in square around the filtration area. c) Visualisation of coordinate system of SII membranes. d) SEM scan of pore structure within a hexagon. e) Photograph of the membranes before separation from the wafer. f) Empty sample holder and its backside with voids for magnets in the inset.

The sample holder in Figure S3 is made from stainless steel and contains holes for fixing disk-shaped magnets that may be used to fixate the holder on a magnetic sample table or the sample itself on the holder by adding further magnets as counterparts on top. The holder contains metallic guiding edges that facilitate positioning and prevent sample movement without the need for glues, clamps or screws. Carvings underneath the pore areas assure that air can move freely while inserting the sample. Additionally, there is ample space for picking up the sample with tweezers from the side. This way, samples are handled with minimum risk of breaking the filter, adhesion problems or rapid movements that may lead to particle loss when removing it from its substrate.

### 5. Other substrates

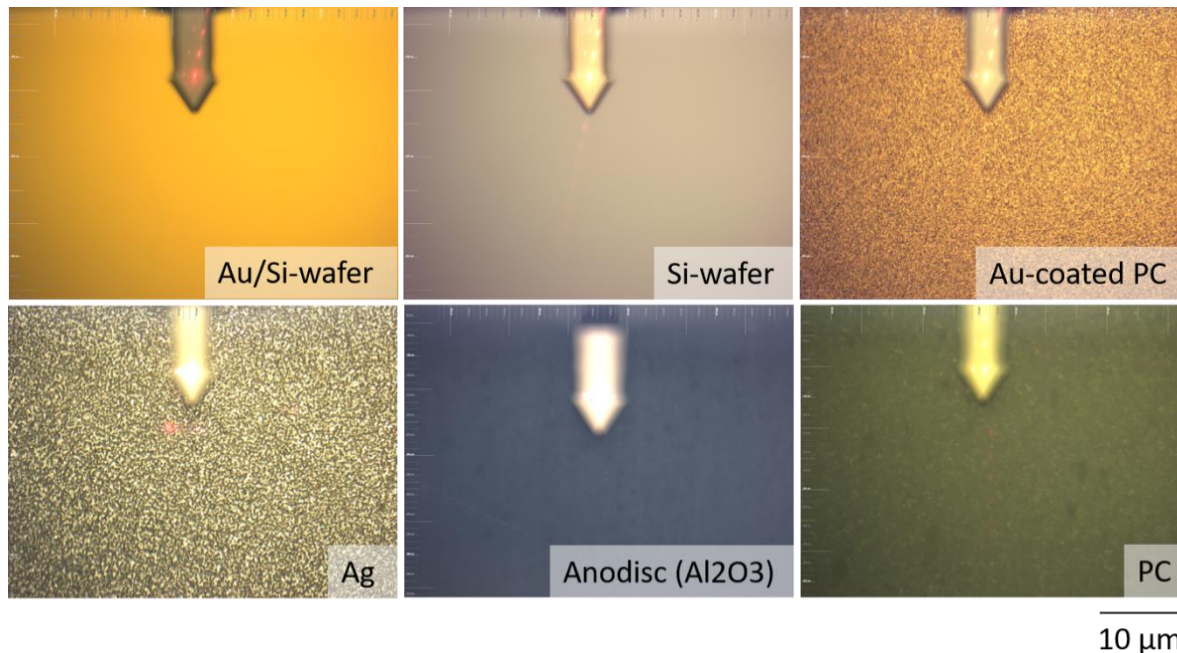


**Figure S4.** Microscope view of commercially available substrates for the submicron fraction in a neasnom set-up applied for nano-FTIR. Common substrates feature no or points for optical orientation and re-location of sampling spots or are rough themselves. Au (100 nm)/Si: ISIT, Si-wafer: ISIT, Au-coated PC (pore 0,4 µm, top 40 nm Au, bottom 20 nm): 2SPI Supplies, Ag pores (0.45 µm): Pieper Filter GmbH, Anodisc pore (0,2 µm): Whatman, PC pore (0.2 µm): Whatman.



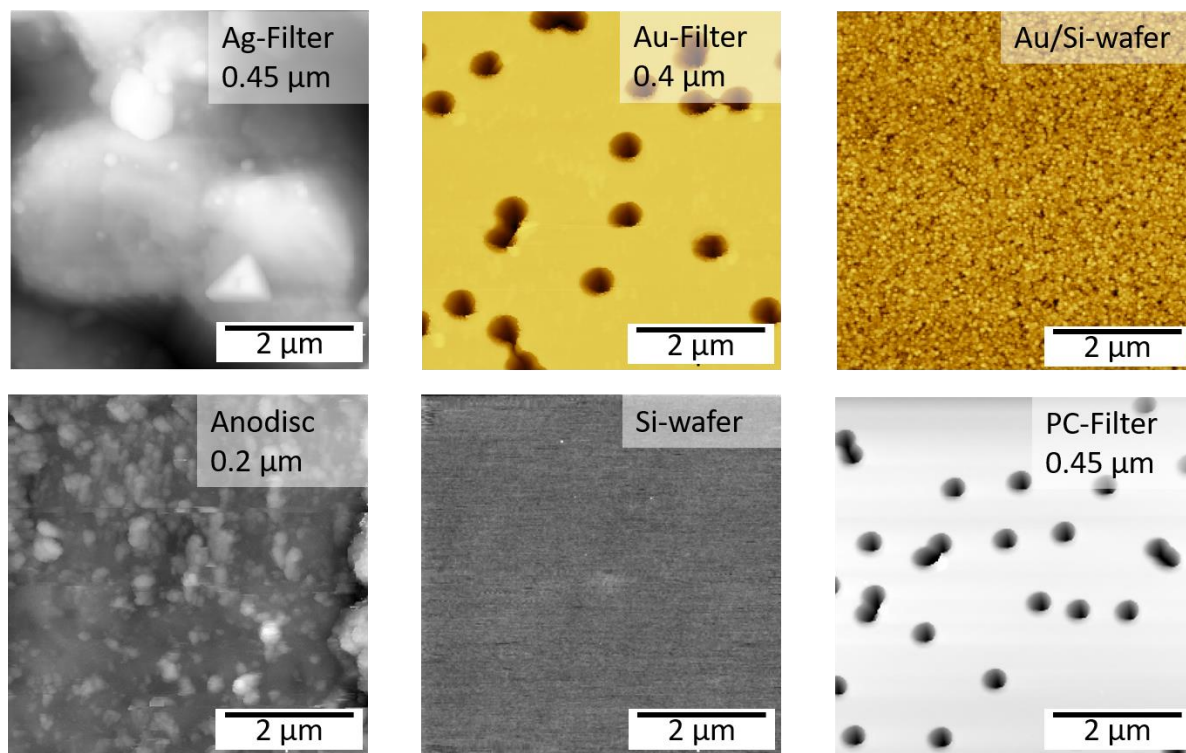


**Figure S5.** Topographic scans of potential substrates for nano-FTIR analysis of nanoscale particles.

## 6. Bow along pore area

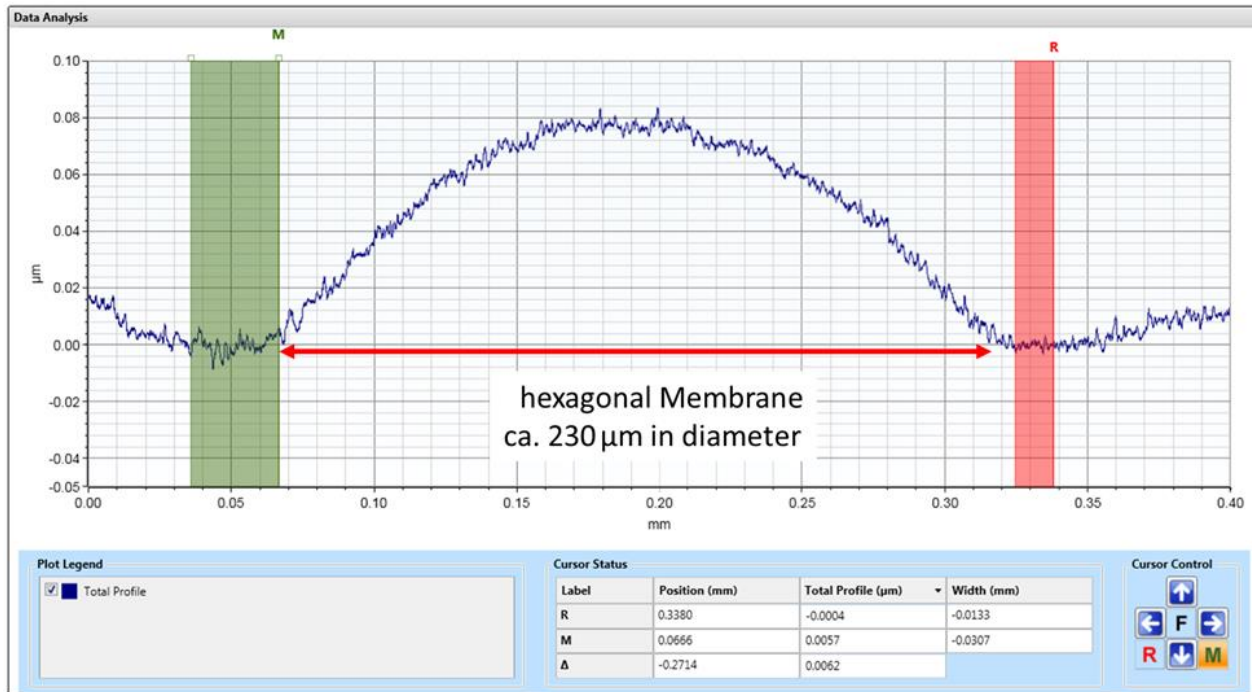


Figure S6. Bow measurement with Bruker Profilometer Dektak XT on finished filter device

## 7. Modified Bosch etching

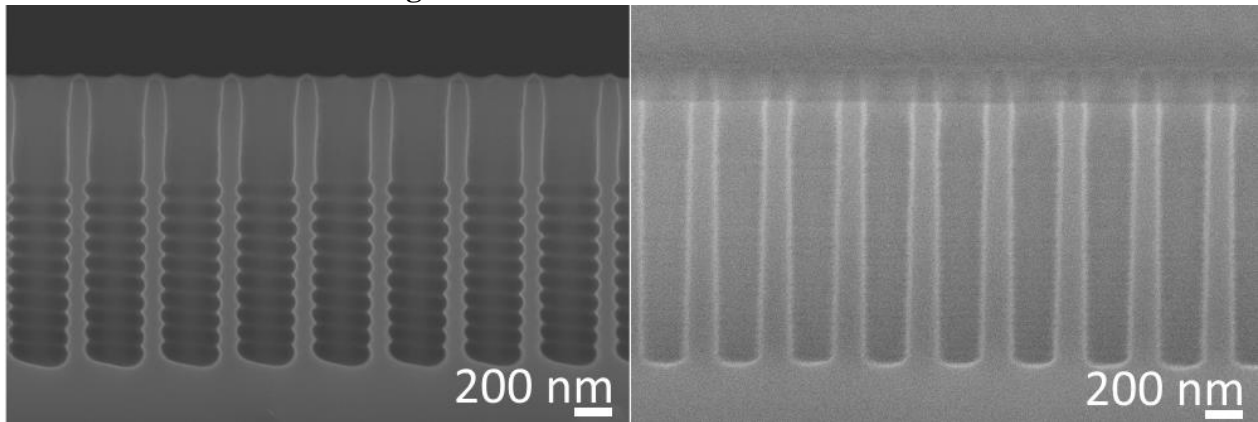
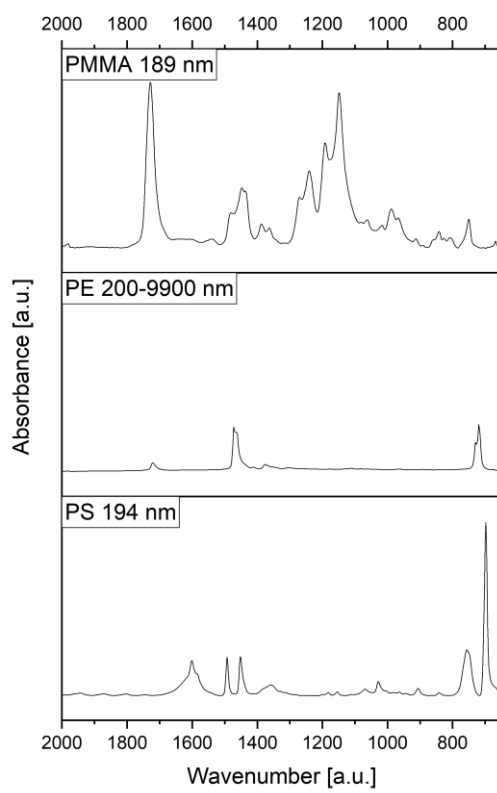


Figure S7. SEM micrographs of membrane cross sections with initial and modified Bosch etching. On the left, after steady state etching, 10 cycles of polymer deposition and etching were carried out to reach ~510 nm (steady state etching) + ~930 nm (Bosch etching) depth. On the right after shorter steady state etching (~320 nm), 25 cycles with modified polymer deposition and etching time were applied for additional ~1070 nm depth. This results in less resist consumption and smooth scalloping.

## 8. ATR-IR Spectra of particle samples



**Figure S8.** ATR-IR spectra of purified and dried aliquots of the polymer particles utilized in this work.



## 9. Raman spectra PE particle and Si membrane filter

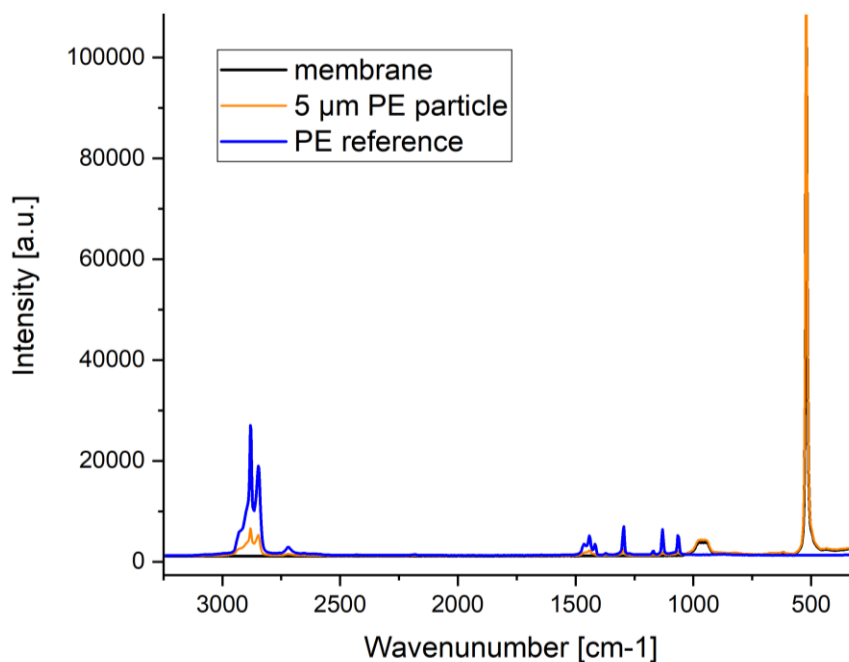


**Figure S9.** Full Raman spectra of 5  $\mu\text{m}$  PE MP particle, pure silicon membrane and PE reference.

## 10. Nano-FTIR and fluorescence spectroscopy

Being able to re-locate spots on the sample, it is possible to combine standard methods, such as fluorescence microscopy for a quick and general examination of a sample, with a detailed examination of nanoscale particles by nano-FTIR, for example to confirm the integrity of particle and fluorescent dye conjugates in translocation or uptake experiments. Not only can fluorescently dyed polymer nanoparticles be utilized in ecotoxicological studies, they may also serve in process control when working with nanoscale particles.

Figure S8 displays microscopic images of a sample accidentally contaminated by internally labelled UV-fluorescent PS plum particles with average diameters of 530 nm. The suspicion of a possible contamination first surfaced in nano-FTIR measurements due to size and spectral information in form of the characteristic two PS peaks between 1500 and 1400  $\text{cm}^{-1}$  and was then confirmed by fluorescent microscopy. The nano-FTIR spectrum of a labelled PS particle in Figure S8c is stitched from two spectra measured with different incident ranges to widen the spectral range to 1750 – 670  $\text{cm}^{-1}$ . A comparison with an ATR-IR spectrum of purified particles from the same batch and a PS database spectrum reveals no significant differences apart from an instrument artefact between 1250 and 1200  $\text{cm}^{-1}$ .

The reason for the cross-contamination was later identified as a lack of mechanical cleaning before inserting the well-rinsed glass funnel, used for filtration, into a cleaning solution in between the preparation of two samples. The problem was solved for further samples by thoroughly wiping the glassware with cotton wool drenched in isopropanol or ethanol after the filtration of samples, followed by chemical cleaning in a cleaning bath (Edisonite solution).

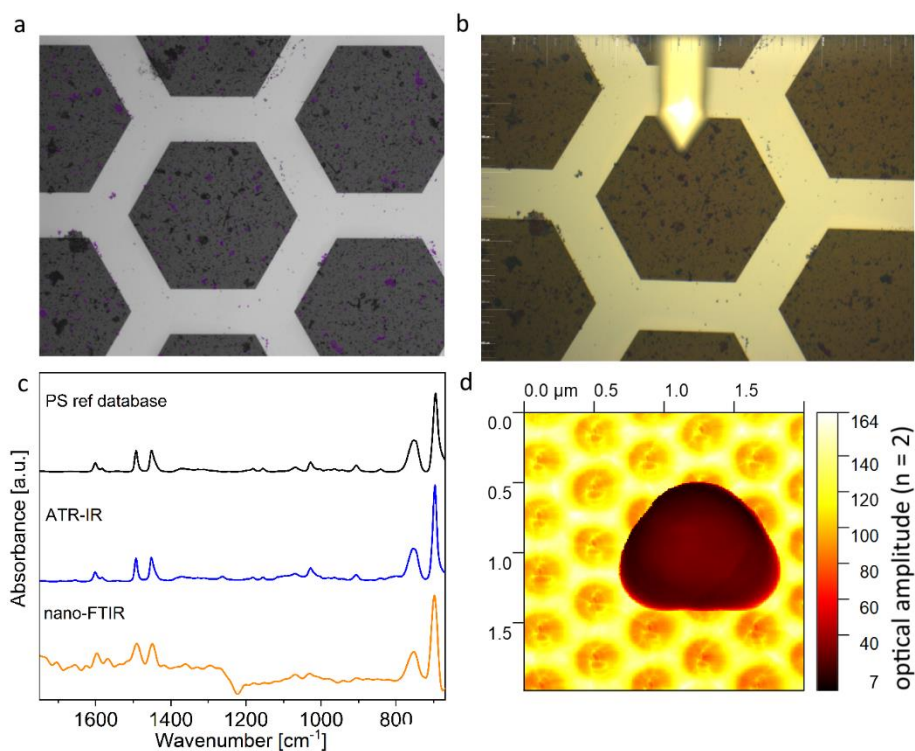


**Figure S10.** a) Overlay of light microscopic and fluorescence (excitation 385 nm) micrographs at 20x magnification; b) the same area in the microscopic view of the neaSNOM top camera. c) nano-FTIR ( $n=2$ ) and ATR-IR spectra of plum color labeled PS particles plotted with a PS database spectrum.<sup>1</sup> The feature below 1250  $\text{cm}^{-1}$  is an instrumental artifact. Spectra were scaled and offset for clarity. d) 2 x 2  $\mu\text{m}$  scan with local optical amplitude data ( $n = 2$ , red: min., yellow: max.).

1. Primpke, S.; Wirth, M.; Lorenz, C.; Gerdtts, G., Reference database design for the automated analysis of microplastic samples based on Fourier transform infrared (FTIR) spectroscopy. *Anal Bioanal Chem* **2018**, *410* (21), 5131-5141; DOI 10.1007/s00216-018-1156-x.